THERMAL DECOMPOSITION REACTIONS OF METAL CARBOXYLATO COMPLEXES IN THE SOLID STATE. III. THERMOGRAPHIC AND DIFFERENTIAL THERMAL STUDIES OF METAL OXALATO, MALONATO AND SUCCINATO COMPLEXES

H.L. SAHA and S. MITRA *

Department of Chemistry, Manipur University, Imphal 795 003 (India)

(Received 21 October 1986)

ABSTRACT

The thermal properties of metal carboxylato complexes of the first transition metals, Mn(II), Fe(II), Fe(III), Co(II), Ni(II) and Cu(II), and non-transition metals, Zn(II) and Cd(II), in the solid state were studied under non-isothermal conditions in a nitrogen atmosphere by simultaneous TG and DTA. TG and DTA curves showed that the decomposition took place in single or multiple steps and thermal stability of the complex decreased, approximately, with the increase of the standard potential of the central metal ion. Thermodynamic parameters, such as activation energy, E_a^*, enthalpy change, ΔH, and entropy change, ΔS, for dehydration and decomposition were determined from TG and DTA curves by standard methods. A linear correlation was found between ΔH and ΔS, and E_a^* and ΔS, in dehydration and decomposition processes. An irreversible phase transition was observed for $Li_2[Co(suc)_2]$ in the DTA curve. The residual products were mixtures of Li_2CO_3 and metal oxides except $Li_2[Mn(ox)_2]$, $Li_2[Zn(mal)_2]$ and $Li_2[Cd(mal)_2]$, where the final products were a mixture of $Li_2O \cdot MnO_2$, $Li_2CO_3 \cdot ZnCO_3$ and $Li_2CO_3 \cdot CdCO_3$, respectively.

INTRODUCTION

Thermal investigations of metal oxalato complexes in the solid state under non-isothermal conditions have been carried out by several researchers [1–9]. However, it has been found that studies on metal malonato and succinato complexes are very scarce [8,9]. Complexes prepared were of the type: $Li_2[ML_2] \cdot nH_2O$ and $Li_3[FeL_3] \cdot nH_2O$, where M = Mn(II), Fe(II), Co(II), Ni(II), Cu(II), Zn(II) and Cd(II), L = oxalate, malonate and succinate ligands and $n = 1$–7. They were characterized by elemental analyses, IR spectral data, and thermal investigations were made under non-isothermal conditions in a nitrogen atmosphere in the solid state.

---

* Author for correspondence.

The conversion $[FeL_3]^{3-} \rightarrow [FeL_2]^{2-}$ occurred by an electron transfer from a coordinated ligand ion to the central metal ion. Some useful conclusions were made from the thermodynamic parameters such as activation energy, E_a^*, enthalpy change, ΔH, and entropy change, ΔS.

EXPERIMENTAL

The complexes of the type, $Li_2[ML_2] \cdot nH_2O$ and $Li_3[FeL_3] \cdot nH_2O$ were synthesized by a general method *. The hydrated metal salt (2.0 mmol) in distilled water (10 cm^3) was mixed with a solution of ligand (40 mmol) in the same solvent (10 cm^3) and the mixture was stirred for $\frac{1}{2}$ h for complete precipitation. The product was collected, washed with water and ethanol and dried in a desiccator (yield $\approx$ 65–70%). The chemicals used were obtained from B.D.H. Certain modifications were made for malonato complexes due to their high solubilities in aqueous media. The complexes were characterized by elemental analyses [10] with standard semimicro techniques (Table 1). The thermogravimetric (TG) and differential thermal analysis (DTA) curves were recorded simultaneously using a Shimadzu DT-30 thermal analyser (Japan) in a constant flow of nitrogen with a Pt-crucible using α-Al$_2$O$_3$ as the standard, keeping the heating rate at $10\,^\circ$C min^{-1} for each run, and using 10–20 mg powdered sample.

Activation energies (E_a^*) were calculated from TG and DTA curves using standard methods. Enthalpy changes (ΔH) were calculated from the DTA peak area using indium metal as the calibrant. IR spectra were recorded in KBr media with a Perkin-Elmer 783 IR spectrometer, and carbon was analysed by a Perkin-Elmer 240 C elemental analyser.

RESULTS AND DISCUSSION

TG and DTA studies

TG and DTA curves of some metal oxalato, malonato and succinato complexes are shown in Figs. 1–3. Cd(II) and Zn(II) complexes of malonate and succinate have no lattice water. The remaining complexes in all the series are trihydrates, except $Li_2[Zn(mal)_2] \cdot H_2O$, $Li_2[Cu(ox)_2] \cdot 2H_2O$, $Li_2[Cd(ox)_2] \cdot 4H_2O$, $Li_2[Fe(suc)_2] \cdot 4H_2O$, $Li_3[Fe(ox)_3] \cdot 6H_2O$, $Li_2[Ni(ox)_2] \cdot 6H_2O$, $Li_2[Cu(mal)_2] \cdot 6H_2O$, $Li_2[Ni(suc)_2] \cdot 6H_2O$, $Li_2[Mn(suc)_2] \cdot 7H_2O$ and $Li_2[Co(suc)_2] \cdot 7H_2O$. All the complexes lost their water molecules before decomposition, except $Li_2[Cu(ox)_2] \cdot 2H_2O$, where dehydration and decomposition occurred simultaneously in a single

---

* For Fe(III) complex the ratio of metal salt to ligand was 1:3.

TABLE 1

Analytical data for metal oxalato (ox), malonato (mal) and succinato (suc) complexes

Compound	Elemental analyses (%) [a]	
	Central metal	Carbon
$Li_2[Mn(ox)_2] \cdot 3H_2O$	18.40 (18.38)	15.98 (16.06)
$Li_2[Fe(ox)_2] \cdot 3H_2O$	18.60 (18.63)	15.96 (16.01)
$Li_3[Fe(ox)_3] \cdot 6H_2O$	12.41 (12.44)	16.00 (16.01)
$Li_2[Co(ox)_2] \cdot 3H_2O$	19.43 (19.46)	15.91 (15.85)
$Li_2[Ni(ox)_2] \cdot 6H_2O$	16.51 (16.46)	13.42 (13.46)
$Li_2[Cu(ox)_2] \cdot 2H_2O$	21.92 (21.95)	16.59 (16.58)
$Li_2[Zn(ox)_2] \cdot 3H_2O$	21.11 (21.13)	15.55 (15.51)
$Li_2[Cd(ox)_2] \cdot 4H_2O$	30.00 (30.02)	12.78 (12.82)
$Li_2[Mn(mal)_2] \cdot 3H_2O$	16.78 (16.81)	22.00 (22.02)
$Li_2[Fe(mal)_2] \cdot 3H_2O$	17.00 (17.04)	21.92 (21.96)
$Li_3[Fe(mal)_3] \cdot 3H_2O$	12.76 (12.78)	24.68 (24.72)
$Li_2[Co(mal)_2] \cdot 3H_2O$	17.78 (17.81)	21.80 (21.76)
$Li_2[Ni(mal)_2] \cdot 3H_2O$	17.71 (17.75)	21.70 (21.77)
$Li_2[Cu(mal)_2] \cdot 6H_2O$	16.28 (16.31)	18.43 (18.48)
$Li_2[Zn(mal)_2] \cdot H_2O$	21.61 (21.69)	23.88 (23.89)
$Li_2[Cd(mal)_2]$	33.99 (34.02)	21.83 (21.79)
$Li_2[Mn(suc)_2] \cdot 7H_2O$	12.81 (12.87)	22.40 (22.49)
$Li_2[Fe(suc)_2] \cdot 4H_2O$	14.92 (14.94)	25.69 (25.68)
$Li_3[Fe(suc)_3] \cdot 3H_2O$	11.63 (11.66)	30.00 (30.07)
$Li_2[Co(suc)_2] \cdot 7H_2O$	13.69 (13.67)	22.21 (22.28)
$Li_2[Ni(suc)_2] \cdot 6H_2O$	14.29 (14.22)	23.30 (23.26)
$Li_2[Cu(suc)_2] \cdot 3H_2O$	17.52 (17.48)	26.38 (26.41)
$Li_2[Zn(suc)_2]$	20.92 (20.99)	30.81 (30.83)
$Li_2[Cd(suc)_2] \cdot 3H_2O$	27.21 (27.26)	23.21 (23.28)

[a] Figures in parentheses are calculated values.

step (Fig. 1, Table 2). TG and DTA curves of all the complexes indicated the single step dehydration except, $Li_3[Fe(ox)_3] \cdot 6H_2O$, $Li_2[Cu(mal)_2] \cdot 6H_2O$ and $Li_2[Cd(suc)_2] \cdot 3H_2O$, where multiple peaks were noticed in DTA curves. The temperature ranges and peak temperatures of the dehydration processes are shown in Tables 2–4. The TG curves of oxalato complexes show a single step decomposition (Table 2), except $Li_3[Fe(ox)_3]$ (Fig. 1). A similar phenomenon was also reflected in DTA curves, except $Li_2[Fe(ox)_2]$, $Li_3[Fe(ox)_3]$ and $Li_2[Zn(ox)_2]$, where multiple exothermic peaks were noticed. In malonato and succinato complexes single-step decompositions were followed in TG curves, except $Li_3[Fe(mal)_3]$, $Li_2[Cu(mal)_2]$, $Li_2[Cd(mal)_2]$ and $Li_2[Cd(suc)_2]$, where two-stage decompositions were found. The corresponding DTA curves of malonato and succinato complexes showed multiple peaks, except $Li_2[Co(mal)_2]$, $Li_2[Zn(mal)_2]$ and $Li_2[Co(suc)_2]$, where a single peak appeared (Tables 3 and 4). The decomposition of $Li_2[Cu(mal)_2]$ was, however, unique, in view of its decomposition through an unstable intermediate, $Li_2[Cu_2(mal)_2]$, where copper was stated to be univalent [11].
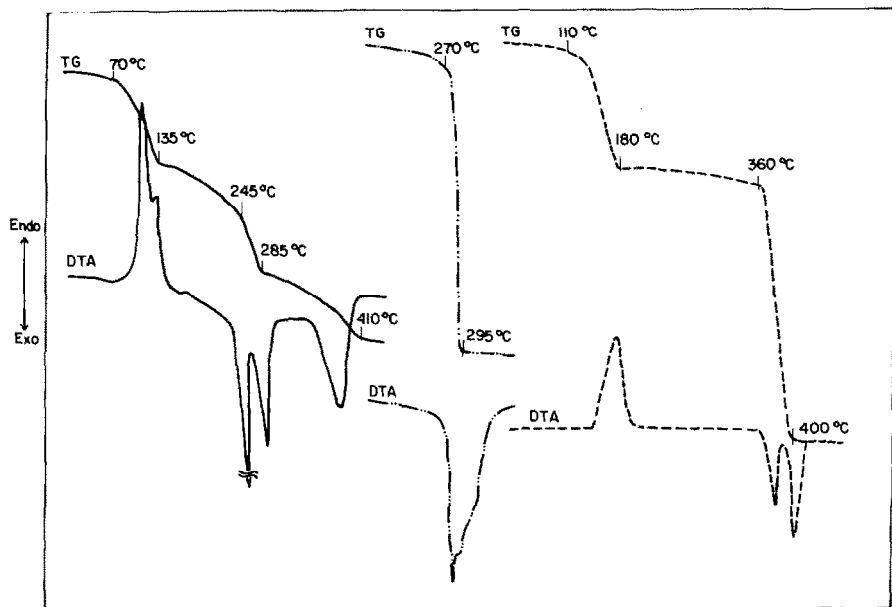
Fig. 1. Thermal curves of $Li_3[Fe(ox)_3] \cdot 6H_2O$, sample mass 9.85 mg (———), $Li_2[Cu(ox)_2] \cdot 2H_2O$, sample mass 17.00 mg ($\cdots-\cdots-\cdots-$) and $Li_2[Zn(ox)_2] \cdot 3H_2O$, sample mass 18.30 mg (- - - - - -).
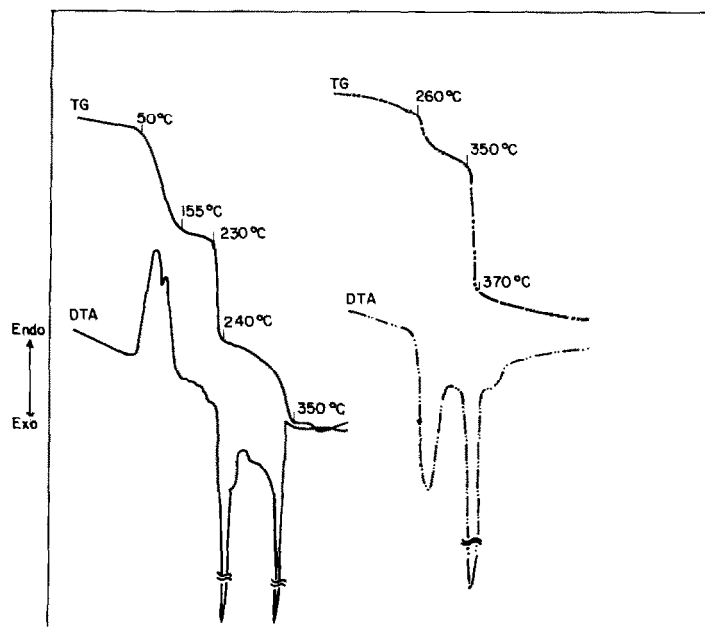
Fig. 2. Thermal curves of $Li_2[Cu(mal)_2] \cdot 6H_2O$, sample mass 11.53 mg (———) and $Li_2[Cd(mal)_2]$, sample mass 14.80 mg ($\cdots-\cdots-\cdots-$).

TABLE 2

Dehydration and decomposition reactions of metal oxalato complexes

No.	Decomposition reaction	Temperature range (°C)	DTA peak temperature (°C)		$E_a^{\star}$ (kJ mol^{-1})		ΔH (kJ mol^{-1})	ΔS (J K^{-1} mol^{-1})
			Endo.	Exo.	TG	DTA		
1	Li$_2$[Mn(C$_2$O$_4$)$_2$]·3H$_2$O → Li$_2$[Mn(C$_2$O$_4$)$_2$]	140–210	190		86.8	82.7	45.1	97.4
	Li$_2$[Mn(C$_2$O$_4$)$_2$] → Li$_2$O·MnO$_2$	270–335		330	170.1	130.4	102.4	175.7
2	Li$_2$[Fe(C$_2$O$_4$)$_2$]·3H$_2$O → Li$_2$[Fe(C$_2$O$_4$)$_2$]	150–220	200		120.3	129.0	128.5	271.7
	Li$_2$[Fe(C$_2$O$_4$)$_2$] → Li$_2$CO$_3$·FeO	220–275		225, 255	–	–	–	–
3	Li$_3$[Fe(C$_2$O$_4$)$_3$]·6H$_2$O → Li$_3$[Fe(C$_2$O$_4$)$_3$]	70–135	110,130		63.0	–	197.8 [a]	–
	Li$_3$[Fe(C$_2$O$_4$)$_3$] → Li$_2$[Fe(C$_2$O$_4$)$_2$]	135–245		245	38.2	–	–	–
	Li$_2$[Fe(C$_2$O$_4$)$_2$] → Li$_2$[Fe(C$_2$O$_4$)$_{1\frac{1}{2}}$]	245–285		285	219.4	–	–	–
	Li$_2$[Fe(C$_2$O$_4$)$_{1\frac{1}{2}}$] → Li$_2$CO$_3$·FeO	285–410		380	109.9	109.9	74.0	113.3
4	Li$_2$[Co(C$_2$O$_4$)$_2$]·3H$_2$O → Li$_2$[Co(C$_2$O$_4$)$_2$]	150–200	190		143.2	122.6	50.0	107.9
	Li$_2$[Co(C$_2$O$_4$)$_2$] → Li$_2$CO$_3$·CoO	290–310		300	246.0	147.4	91.4	159.6
5	Li$_2$[Ni(C$_2$O$_4$)$_2$]·6H$_2$O → Li$_2$[Ni(C$_2$O$_4$)$_2$]	80–160	125		66.7	61.6	94.4	239.6
	Li$_2$[Ni(C$_2$O$_4$)$_2$] → Li$_2$CO$_3$·NiO	345–380		370	338.2	220.0	68.4	106.4
6	Li$_2$[Cu(C$_2$O$_4$)$_2$]·2H$_2$O → Li$_2$CO$_3$·CuO	270–295		280, 290	–	–	54.2 [a]	–
7	Li$_2$[Zn(C$_2$O$_4$)$_2$]·3H$_2$O → Li$_2$[Zn(C$_2$O$_4$)$_2$]	110–180	175		88.7	116.0	46.5	106.1
	Li$_2$[Zn(C$_2$O$_4$)$_2$] → Li$_2$CO$_3$·ZnO	360–400		375, 395	486.7	–	24.5 [a]	–
8	Li$_2$[Cd(C$_2$O$_4$)$_2$]·4H$_2$O → Li$_2$[Cd(C$_2$O$_4$)$_2$]	70–135	115		79.0	105.4	62.1	160.1
	Li$_2$[Cd(C$_2$O$_4$)$_2$] → Li$_2$CO$_3$·CdO	295–355		340	335.2	240.0	42.5	71.0

[a] Overall enthalpy change.
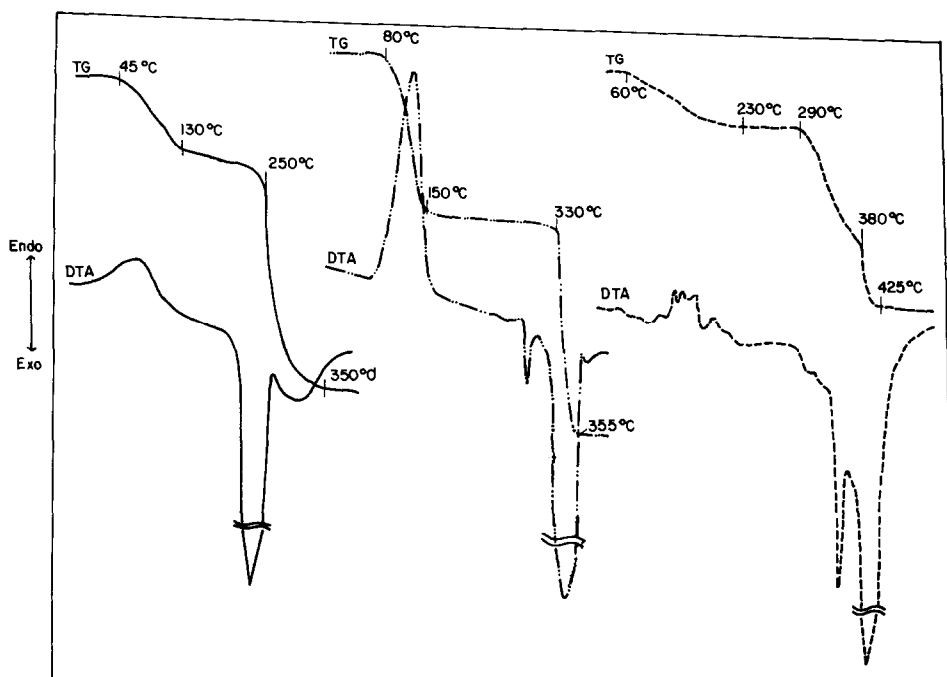
Fig. 3. Thermal curves of $Li_3[Fe(suc)_3] \cdot 3H_2O$, sample mass 11.50 mg (———), $Li_2[Co(suc)_2] \cdot 7H_2O$, sample mass 14.80 mg ($\cdot\cdot-\cdot\cdot-\cdot\cdot-$) and $Li_2[Cd(suc)_2] \cdot 3H_2O$, sample mass 10.75 mg (- - - - - -).

For the DTA curve of $Li_2[Co(suc)_2]$ a prominent phase transition was observed (exothermic in nature) showing no weight loss along the TG curve ($280–300°C$). Such a phase change in the DTA curve indicates that some sort of structural rearrangement is occurring before the decomposition of the complex.

The transformation of the tris- to the bis-oxalato complex suggested the reaction to be:

$$Li_3[Fe(C_2O_4)_3] \rightarrow Li_2[Fe(C_2O_4)_2] + \tfrac{1}{2}Li_2C_2O_4 + CO_2 \qquad (1)$$
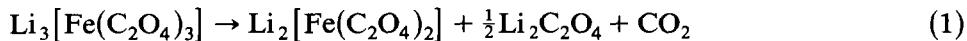
The liberation of CO_2 indicated that the central metal ion captured an electron from the ligand ion [2]. A similar sequence was also found in the malonato complex, and the respective DTA peak temperatures were 225 and $230°C$. For $Li_3[Fe(suc)_3]$, the intermediate reduction step was not obtained due to its direct conversion to $Li_2CO_3 \cdot FeO$.

For oxalato, malonato and succinato complexes the dehydration peak temperature in either a single step or in the first step of multiple step processes are in the order: Fe(II) > Mn(II) ≈ Co(II) > Zn(II) > Ni(II) > Cd(II) > Fe(III), Ni(II) > Co(II) > Mn(II) ≈ Fe(II) > Cu(II) > Zn(II) > Fe(III) and Ni(II) > Co(II) > Fe(II) > Mn(II) > Cd(II) > Fe(III) ≈ Cu(II), respectively (Tables 2–4) and their respective decomposition peak tempera-

TABLE 3

Dehydration and decomposition reactions of metal malonato complexes

No.	Decomposition reaction	Temperature range (°C)	DTA peak temperature (°C)		$E_a^\star$ (kJ mol⁻¹)		ΔH (kJ mol⁻¹)	ΔS (J K⁻¹ mol⁻¹)
			Endo	Exo.	TG	DTA		
1	$Li_2[Mn(C_3H_2O_4)_2]\cdot 3H_2O \rightarrow Li_2[Mn(C_3H_2O_4)_2]$	150–210	185		128.2	149.2	256.8	560.8
	$Li_2[Mn(C_3H_2O_4)_2] \rightarrow Li_2CO_3\cdot MnO_2$	280–360		275, 300, 350	196.9	–	397.2 [a]	–
2	$Li_2[Fe(C_3H_2O_4)_2]\cdot 3H_2O \rightarrow Li_2[Fe(C_3H_2O_4)_2]$	60–210	185		55.9	64.4	59.7	130.3
	$Li_2[Fe(C_3H_2O_4)_2] \rightarrow Li_2CO_3\cdot FeO$	210–310		240, 270, 300	301.1	–	480.9 [a]	–
3	$Li_3[Fe(C_3H_2O_4)_3]\cdot 3H_2O \rightarrow Li_3[Fe(C_3H_2O_4)_3]$	30–170	80		35.2	39.6	71.4	206.3
	$Li_3[Fe(C_3H_2O_4)_3] \rightarrow Li_2[Fe(C_3H_2O_4)_2]$	170–230		230	70.9	–	–	–
	$Li_2[Fe(C_3H_2O_4)_2] \rightarrow Li_2CO_3\cdot FeO$	230–340		285	76.4	–	–	–
4	$Li_2[Co(C_3H_2O_4)_2]\cdot 3H_2O \rightarrow Li_2[Co(C_3H_2O_4)_2]$	150–210	200		133.4	127.3	139.8	298.7
	$Li_2[Co(C_3H_2O_4)_2] \rightarrow Li_2CO_3\cdot CoO$	280–360		340	241.9	144.9	239.9	399.8
5	$Li_2[Ni(C_3H_2O_4)_2]\cdot 3H_2O \rightarrow Li_2[Ni(C_3H_2O_4)_2]$	200–250	240		152.4	173.2	120.7	235.3
	$Li_2[Ni(C_3H_2O_4)_2] \rightarrow Li_2CO_3\cdot NiO$	310–347		325, 340	392.0	–	483.2 [a]	–
6	$Li_2[Cu(C_3H_2O_4)_2]\cdot 6H_2O \rightarrow Li_2[Cu(C_3H_2O_4)_2]$	50–155	140, 150		51.1	–	155.3	–
	$Li_2[Cu(C_3H_2O_4)_2] \rightarrow Li_2[Cu_2(C_3H_2O_4)_2]$	230–240		230	–	–	–	–
	$Li_2[Cu_2(C_3H_2O_4)_2] \rightarrow Li_2CO_3\cdot CuO$	240–350		320	79.5	–	–	–
7	$Li_2[Zn(C_3H_2O_4)_2]\cdot H_2O \rightarrow Li_2[Zn(C_3H_2O_4)_2]$	115–155	130		72.5	94.3	28.1	69.8
	$Li_2[Zn(C_3H_2O_4)_2] \rightarrow Li_2CO_3\cdot ZnCO_3$	310–350	320	340	401.8	–	–	–
8	$Li_2[Cd(C_3H_2O_4)_2] \rightarrow Li_2[Cd(C_3H_2O_4)_3]_{\frac{3}{2}}$	260–350		300	33.6	46.4	90.4	159.2
	$Li_2[Cd(C_3H_2O_4)_3^{\frac{3}{2}}] \rightarrow Li_2CO_3\cdot CdCO_3$	350–370		360	–	–	–	–

[a] Overall enthalpy change.

TABLE 4

Dehydration and decomposition reactions of metal succinato complexes

No.	Decomposition reaction	Temperature range (°C)	DTA peak temperature (°C)		$E_a^\star$ (kJ mol^{-1})		ΔH (kJ mol^{-1})	ΔS (J K^{-1} mol^{-1})
			Endo.	Exo.	TG	DTA		
1	$Li_2[Mn(C_4H_4O_4)_2]\cdot 7H_2O \rightarrow Li_2[Mn(C_4H_4O_4)_2]$	35–140	105		84.8	77.3	169.5	448.3
	$Li_2[Mn(C_4H_4O_4)_2] \rightarrow Li_2CO_3\cdot MnO_2$	330–370		320, 365	121.7	–	–	–
2	$Li_2[Fe(C_4H_4O_4)_2]\cdot 4H_2O \rightarrow Li_2[Fe(C_4H_4O_4)_2]$	30–140	110		44.5	144.9	98.4	256.8
	$Li_2[Fe(C_4H_4O_4)_2] \rightarrow Li_2CO_3\cdot FeO$	270–470		285, 295	32.6	–	370.0 [a]	–
3	$Li_3[Fe(C_4H_4O_4)_3]\cdot 3H_2O \rightarrow Li_3[Fe(C_4H_4O_4)_3]$	45–130	90		38.8	23.9	162.7	454.4
	$Li_3[Fe(C_4H_4O_4)_3] \rightarrow Li_2CO_3\cdot FeO$	250–350		285, 330	104.0	–	–	–
4	$Li_2[Co(C_4H_4O_4)_2]\cdot 7H_2O \rightarrow Li_2[Co(C_4H_4O_4)_2]$	80–150	120		69.8	96.6	273.9	696.9
	$Li_2[Co(C_4H_4O_4)_2] \xrightarrow{\text{Phase change}} Li_2[Co(C_4H_4O_4)_2]$	280–300		290	–	–	20.8	–
5	$Li_2[Co(C_4H_4O_4)_2] \rightarrow Li_2CO_3\cdot CoO$	330–355		345	219.2	–	–	–
	$Li_2[Ni(C_4H_4O_4)_2]\cdot 6H_2O \rightarrow Li_2[Ni(C_4H_4O_4)_2]$	100–165	140		95.3	99.1	469.2	1136.2
	$Li_2[Ni(C_4H_4O_4)_2] \rightarrow Li_2CO_3\cdot NiO$	370–400		375, 385, 395	486.2	–	757.8 [a]	–
6	$Li_2[Cu(C_4H_4O_4)_2]\cdot 3H_2O \rightarrow Li_2[Cu(C_4H_4O_4)_2]$	45–100	90		68.6	77.0	96.3	265.3
	$Li_2[Cu(C_4H_4O_4)_2] \rightarrow Li_2CO_3\cdot CuO$	265–330		320, 325	364.8	–	333.2 [a]	–
7	$Li_2[Zn(C_4H_4O_4)_2] \rightarrow Li_2CO_3\cdot ZnO$	400–515		440, 490	243.5	–	689.7 [a]	–
8	$Li_2[Cd(C_4H_4O_4)_2]\cdot 3H_2O \rightarrow Li_2[Cd(C_4H_4O_4)_2]$	60–230	100, 120, 135, 160, 185, 210		24.6	–	–	–
	$Li_2[Cd(C_4H_4O_4)_2] \rightarrow Li_2[Cd(C_4H_4O_4)]$	290–380		310, 335, 355	110.7	–	–	–
	$Li_2[Cd(C_4H_4O_4)] \rightarrow Li_2CO_3\cdot CdO$	380–425		395, 420	477.6	–	–	–

[a] Overall enthalpy change.

tures * follow the trend: $Zn(II) > Ni(II) > Cd(II) > Mn(II) > Co(II) > Fe(III) > Fe(II)$, $Co(II) \approx Zn(II) > Ni(II) > Cd(II) > Mn(II) > Fe(II) > Fe(III) \approx Cu(II)$ and $Zn(II) > Ni(II) > Co(II) > Mn(II) \approx Cu(II) > Cd(II) > Fe(II) \approx Fe(III)$.

Activation energies ($E_a^\star$) for dehydration and decomposition were computed from TG curves by Horowitz and Metzger's method [12] and from DTA curves by Borchardt and Daniels' equation [13]. The values are given in Tables 2–4. In most cases values are fairly close to each other, except $Li_2[Ni(mal)_2] \cdot 3H_2O$, $Li_2[Zn(ox)_2] \cdot 3H_2O$ and $Li_2[Fe(suc)_2] \cdot 4H_2O$. Activation energies ($E_a^\star$) for dehydration from DTA curves of oxalato, malonato and succinato complexes follow the sequence: $Fe(II) > Co(II) > Zn(II) > Cd(II) > Mn(II) > Ni(II)$, $Ni(II) > Mn(II) > Co(II) > Zn(II) > Fe(II) > Fe(III)$ and $Fe(II) > Ni(II) > Co(II) > Mn(II) \approx Cu(II) > Fe(III)$, respectively. For decomposition, activation energies ($E_a^\star$) from TG ** curves of oxalato, malonato and succinato complexes follow the order: $Zn(II) > Ni(II) > Cd(II) > Co(II) > Mn(II) > Fe(III)$, $Zn(II) > Ni(II) > Fe(II) > Co(II) > Mn(II) > Fe(III)$ and $Ni(II) > Cu(II) > Zn(II) > Co(II) > Mn(II) > Cd(II) > Fe(III) > Fe(II)$, respectively.

For dehydration, the enthalpy changes (ΔH) and entropy changes (ΔS) of oxalato and malonato complexes were in the order: $Fe(III) > Fe(II) > Ni(II) > Cd(II) > Cu(II)$ *** $> Co(II) > Zn(II) > Mn(II)$ and $Mn(II) > Cu(II) > Co(II) > Ni(II) > Cd(II) > Fe(III) > Fe(II) > Zn(II)$, except the position of Cd(II) and Fe(III) is reversed for entropy changes (ΔS) for the malonato series. In the succinato series, the respective order of enthalpy changes (ΔH) and entropy changes (ΔS) are as follows: $Ni(II) > Co(II) > Mn(II) > Fe(III) > Fe(II) > Cu(II)$ and $Ni(II) > Co(II) > Fe(III) > Mn(II) > Cu(II) > Fe(II)$.

Activation energies (evaluated from TG curves [†]) for decomposition of the oxalato and malonato series follow the order: $Zn(II) > Ni(II) > Cd(II) > Fe(II) > Co(II) > Mn(II) > Fe(III)$, and for the succinato series the order is $Ni(II) > Cu(II) > Zn(II) > Co(II) > Mn(II) > Cd(II) > Fe(III) > Fe(II)$.

The enthalpy changes (ΔH) and entropy changes (ΔS) for decomposition processes of oxalato complexes follow the order: $Mn(II) > Co(II) > Ni(II) > Cd(II) > Zn(II)$. The overall enthalpy changes for malonato and succinato complexes follow the trend: $Ni(II) > Fe(II) > Mn(II) > Co(II)$ and $Ni(II) > Zn(II) > Fe(II) > Cu(II)$, respectively. The order of entropy changes (ΔS) was not evaluated for the multiple peaks in DTA curves.

---

* First peak is considered for multiple steps of decomposition.
** As DTA values were not available.
*** Overall enthalpy change.
[†] $E_a^\star$ from TG curves were considered as very few values from DTA curves were available.
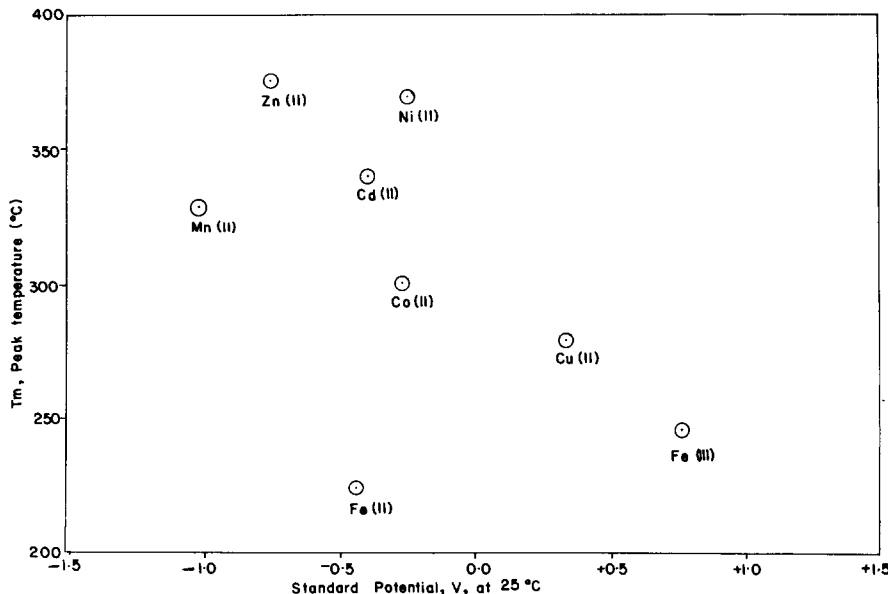
Fig. 4. Plots of peak temperatures (T_m, °C) of decomposition for metal oxalato complexes versus standard potentials, V, of central metal ion at 25°C.
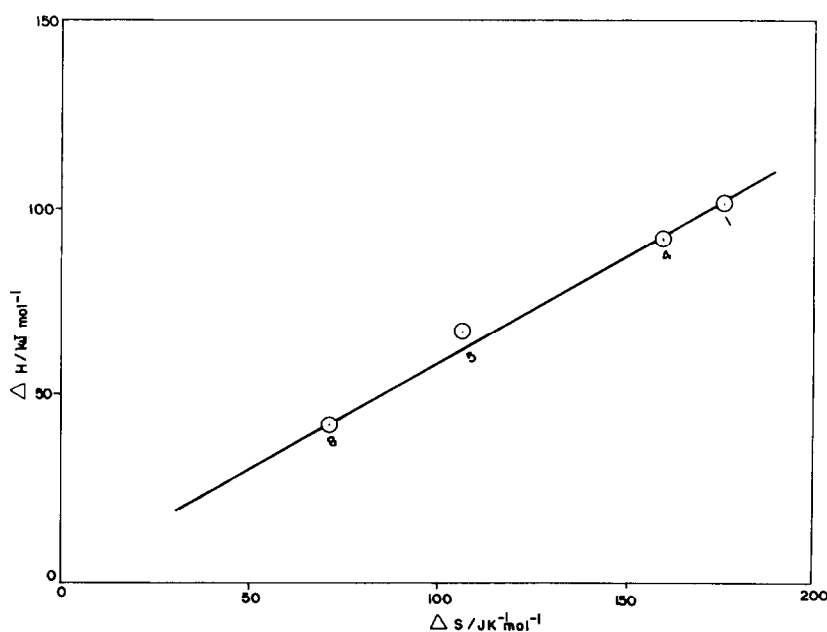

Fig. 5. Plots of ΔH versus ΔS for the thermal decomposition of metal oxalato complexes, 1 = Mn(II), 4 = Co(II), 5 = Ni(II) and 8 = Cd(II).
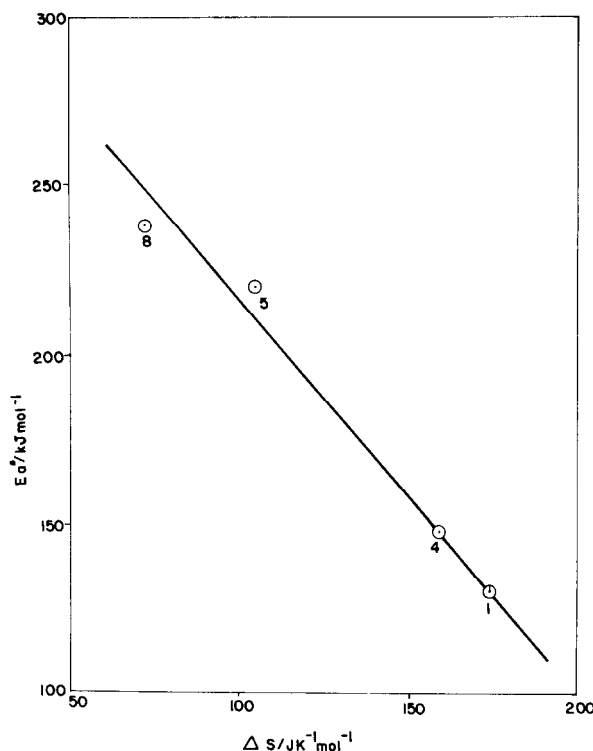
Fig. 6. Plots of $E_a^{\star}$ versus ΔS for the thermal decomposition of metal oxalato complexes, 1 = Mn(II), 4 = Co(II), 5 = Ni(II) and 8 = Cd(II).

By plotting DTA peak temperature (T_m, °C) for decomposition of oxalato complexes against the standard potential of the central metal ions * (Fig. 4), it was found that the thermal stability of the complex decreases, approximately, with the increase in the tendency of the central metal ion to capture an electron from the ligand.

A linear correlation was found by plotting ΔH versus ΔS, as shown in Fig. 5. The values of entropy changes (ΔS) were calculated by the relation [15]:

$$\Delta S = \Delta H / T_m \qquad (2)$$

where T_m is the peak temperature of decomposition in the DTA curves. Similarly, a linear relationship was also observed by plotting $E_a^{\star}$ versus ΔS,

---

* The plots of DTA peak temperatures of the complexes versus the standard potential [14] of the central metal ion forming an aquo complex are given in Fig. 4. These potentials were considered in order to measure the tendency of the central metal ion to capture an electron from the ligand forming an oxalato complex, since the Dq value of H_2O is near to that of $C_2O_4^{2-}$.

as shown in Fig. 6. It has been observed that a system having higher entropy change (ΔS) will require less activation energy ($E_a^\star$) for its decomposition. A more or less similar sequence was also observed for dehydration processes.

REFERENCES

1 N. Tanaka and K. Sato, Bull. Chem. Soc. Jpn., 43 (1970) 789.
2 K. Nagase, Bull. Chem. Soc. Jpn., 45 (1972) 2166.
3 W.W. Wendlandt and E.L. Simmons, J. Inorg. Nucl. Chem., 27 (1965) 2317, 2325.
4 N. Tanaka and M. Nanjo, Bull. Chem. Soc. Jpn., 40 (1967) 330.
5 W.W. Wendlandt and E.L. Simmons, J. Inorg. Nucl. Chem., 28 (1968) 2420.
6 G.M. Bancroft, K.G. Dharmawardena and A.G. Maddock, J. Inorg. Nucl. Chem. Lett., 6 (1970) 403.
7 J.D. Danforth and J. Dix, Inorg. Chem., 10 (1971) 1623.
8 H.L. Saha and S. Mitra, Thermochim. Acta, 109 (1987) 331.
9 H.L. Saha and S. Mitra, Thermochim. Acta, 112 (1987) 275.
10 A.I. Vogel, A Text Book of Quantitative Inorganic Analysis, 3rd edn., Longmans, London, 1968.
11 M.D. Judd, B.A. Plunkett and M.I. Pope, J. Therm. Anal., 6 (1974) 555.
12 H.H. Horowitz and G. Metzger, Anal. Chem., 35 (1963) 1464.
13 H.J. Borchardt and F. Daniels, J. Am. Chem. Soc., 79 (1957) 4141.
14 W.M. Latimer, The Oxidation State of the Elements and Their Potentials in Aqueous Solution, Prentice-Hall, New York, 1952.
15 R. Roy, M. Chaudhuri, S.K. Mandal and K. Nag, J. Chem. Soc., Dalton Trans., (1984) 1681.